

Detailed Description of Research Performed

The Synthesis of Superheavy Nuclei Using Damped Collisions—A Test

In Figure 1, we show the current situation with regard to the synthesis of superheavy nuclei using cold fusion and hot fusion reactions. For cold fusion syntheses, the production cross sections decrease with increasing atomic number of the completely fused system, Z_{CN} , until one reaches element 113 where the measured fusion cross section is 32 fb, a production rate of about 1 atom/year. Even with the modest expected increase in production cross section for element 114, further use of this path to the superheavy nuclei will require significant technical advances.

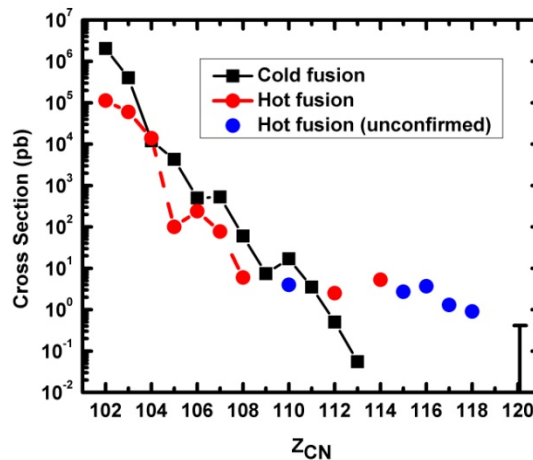


Figure 1. Measured cross sections for the production of the heaviest elements.

For syntheses involving hot fusion reactions, the cross sections decrease significantly from $Z=102$ to $Z=110$ and then decrease more slowly until $Z=118$ where the production cross section is 0.5 pb. Attempts to synthesize element 120 by the $^{64}\text{Ni} + ^{238}\text{U}$ reaction and the $^{58}\text{Fe} + ^{244}\text{Pu}$ reaction have resulted in upper limit cross sections of about 0.1 pb and 0.4 pb, respectively. [1, 2]. In view of this situation, there has been a revival of interest in the use of damped collisions of massive nuclei at near barrier energies to synthesize superheavy nuclei, particularly those nuclei with large neutron excess, approaching the $N=184$ shell. In the 1980s [3] there were attempts to use the $^{238}\text{U} + ^{238}\text{U}$ and the $^{238}\text{U} + ^{248}\text{Cm}$ reactions at above barrier energies to produce trans-target nuclides. While there was evidence for the formation of neutron-rich isotopes of Fm and Md at the $0.1 \mu\text{b}$ level, no higher actinides were found. The fundamental problem was that the nuclei that were produced far above the target nucleus were the result of events with high total kinetic energy loss, i.e., high excitation energies and resulting poor survival probabilities. Very recently, Zagrebaev and Greiner [4, 5, 7-12] using a new model [6] for these collisions, have examined the older experiments and some proposed new experiments ($^{232}\text{Th} + ^{250}\text{Cf}$, $^{238}\text{U} + ^{238}\text{U}$, and $^{238}\text{U} + ^{248}\text{Cm}$). With their new model which emphasizes the role of shell effects in damped collisions, they are able to correctly describe the previously measured fragment angular, energy and charge distributions from the ^{136}Xe

+ ^{209}Bi reaction and the isotopic yields of Cf, Es, Fm and Md from the $^{238}\text{U} + ^{248}\text{Cm}$ reaction. They predict that by a careful choice of beam energies and projectile-target combinations, one might be able to produce n-rich isotopes of element 112 in the $^{248}\text{Cm} + ^{250}\text{Cf}$ reaction. They suggest the detection of $^{267, 268}\text{Db}$ and $^{272, 271}\text{Bh}$ (at the pb level) in the Th + Cf or U + Cm reactions to verify these predictions. Such experiments are very difficult because of the low cross sections, the lower intensities of these massive projectile beams and the problems of detecting the reaction products in an ocean of elastically scattered particles, etc.

However, in 2007, Zagrebaev and Greiner [13] outlined a simpler test of their theoretical predictions. They applied the same model used to study the U + Cm, Th + Cf and U + U collisions to the $^{160}\text{Gd} + ^{186}\text{W}$ reaction. The predicted mass yield distributions and the yields of the Pb transfer products ($\Delta Z = + 8$) are shown in Figure 2. The predicted mass yields range from 1-100 mb while the Pb isotopic yields range from 1-5 mb. Based upon our prior experience of determining fragment mass and isotopic distributions in the reaction of low energy, intermediate energy and relativistic heavy ions with Ta, Au and Pb, we concluded that these same quantities could be determined in the reaction of 856 MeV ^{160}Gd with ^{186}W .

The experiment took place in the ATSCAT chamber at the ATLAS facility at the Argonne National Laboratory. A beam of 960 MeV ^{160}Gd struck a 5.775 mg/cm^2 foil of ^{186}W (99 percent enriched) mounted at the center of the chamber. The center of target beam energy was 859 MeV ($E_{c.m.} = 461.9 \text{ MeV}$). A deep suppressed Faraday cup at the exit of the chamber was used to monitor the beam intensity. The average on-target projectile intensity was 70 enA of $^{160}\text{Gd}^{34+}$. The foil was irradiated for 19 hours. The target-catcher foil assembly is shown schematically in Figure 3. Recoiling reaction products were collected using either 9.7 mg/cm^2 Mylar foils or 13.5 mg/cm^2 Al foils that should stop all reaction products. The primary beam passed through a hole in the center of the catcher foil apparatus. After irradiation, the catcher foils were divided into three samples, "backward", "forward", and "side" corresponding to angular cuts of $90\text{-}180^\circ$, $9\text{-}17^\circ$, and $17\text{-}90^\circ$, respectively. For each of these angular cuts, there are two samples, Mylar and Al, corresponding to azimuthal angles of $0\text{-}180^\circ$ and $180\text{-}360^\circ$. Gamma ray spectroscopy of the Mylar catcher foil samples and the ^{186}W target was carried out using a well calibrated Ge detector in the ATLAS hot chemistry laboratory. The total observation period was 11 days in which about 15 measurements of each sample were made. The Al catcher foils were dissolved in mineral acid and the

Pb isotopes were separated from the solution. [14]. Following chemical separation, the Pb isotope fraction was counted on the same Ge detector. The analysis of the γ -ray spectra was done using a modified version of the DECHAOS software [15]. 107 radionuclides were identified in the samples. The end of bombardment (EOB) activities of the nuclides were used to calculate production cross sections taking into account the variable beam intensities using standard equations for the growth and decay of radionuclides during irradiation [16].

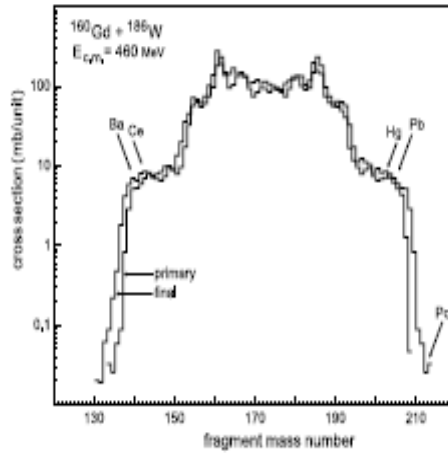
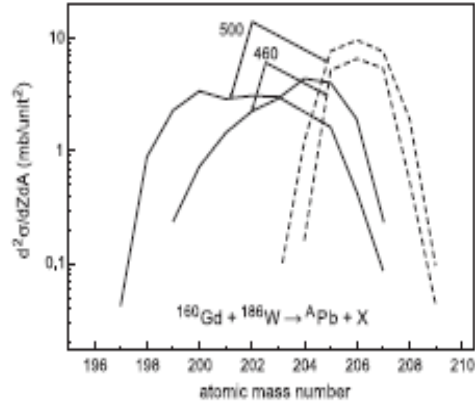


Figure 2. (a) Predicted mass distribution for the products for the $^{160}\text{Gd} + ^{186}\text{W}$ reaction (before and after particle evaporation).

(b) Predicted Pb isotopic distribution for this reaction. The dashed lines show the primary distributions while the solid lines show the final distributions after particle emission.

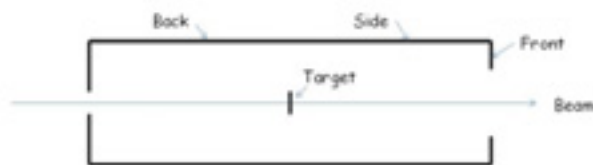


Figure 3. Schematic diagram of experimental apparatus

The first aspect of the Zagrebaev and Greiner predictions for this reaction that can be checked is the Pb isotopic distribution (Fig. 2). No Pb isotopes were detected in the target, catcher foil or chemical fractions. A rough upper limit cross section for the relevant radionuclides (51.9 h ^{203}Pb and 67.2 m $^{204}\text{Pb}^{\text{m}}$) is ~ 0.05 mb. Based upon the predictions shown in Figure 2, the expected cross sections for these radionuclides are ~ 0.06 and 0.2 mb, respectively.

The measured nuclidic formation cross sections were placed in six groups according to mass number. These cross sections were corrected for precursor beta decay, where necessary, by assuming the independent yield cross sections for a given species $\sigma(Z,A)$ can be expressed as a histogram that lies along a Gaussian curve.

$$\sigma(Z,A) = \sigma(A) [2\pi C_Z^2(A)]^{-1/2} \exp\left[\frac{-(Z - Z_{\text{mp}})^2}{2\pi C_Z^2(A)}\right]$$

where $C_Z(A)$ is the Gaussian width parameter for mass number A and $Z_{\text{mp}}(A)$ is the most probable atomic number for that A . Using this assumption and the further assumption that

$\sigma(A)$ varies slowly and smoothly as a function of A [allowing data from adjacent isobars to be combined in determining $Z_{\text{mp}}(A)$ and $C_Z(A)$], one can use the laws of radioactive decay to iteratively correct the measured cumulative formation cross sections for precursor decay. Within each of the six groups, the data were fit to a Gaussian-shaped independent yield distribution. The width parameter was found to be constant over a given range in A while the centers of the charge distributions were adequately represented by linear functions in A over a limited range in A although we expect $Z_{\text{mp}}(A)$ to be non-linear. (Only nuclides with well characterized beta-decay precursors and cases where both members of an isomeric pair were observed were included in the analysis). The isobaric yield distribution obtained from this analysis is shown in Figure 4 along with the predictions of Zagrebaev and Greiner. The error bars on the integrated data points reflect the uncertainties due to counting statistics and those introduced in the charge distribution fitting process which have been estimated to be approximately 25 % [17]. The predicted and calculated mass distributions do not agree although there are some common features. There is a peak in the mass distribution around mass 180 (of differing magnitudes). The trans-target nuclidic yields are greatly lower than predicted and the lighter products ($A \sim 100$) are presumably the fission products from the decay of the target-like fragments. It appears the predicted survival of the trans-target nuclides due to shell effects is not seen.

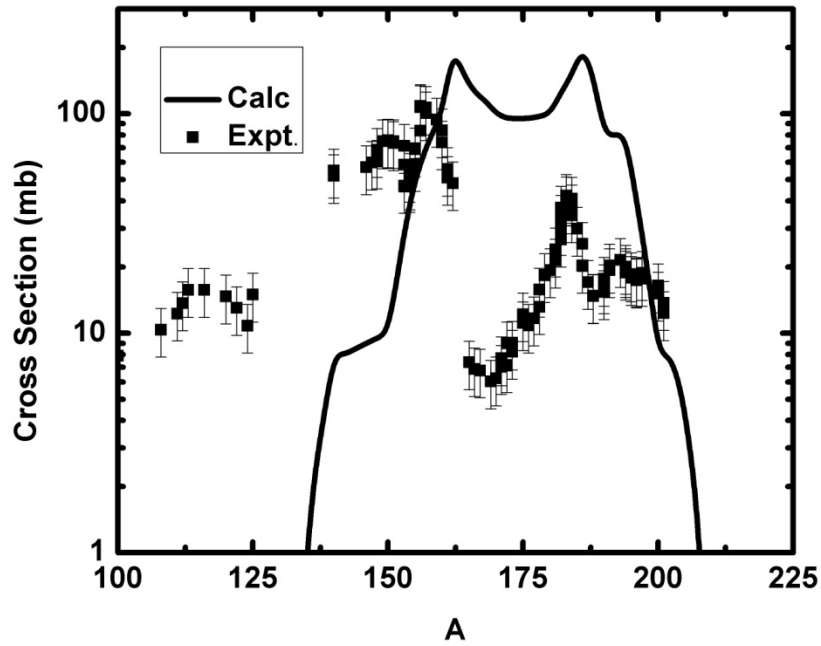


Figure 4. Measured and predicted mass distributions for the $^{160}\text{Gd} + ^{186}\text{W}$ reaction.

Isospin Dependence of Capture Cross Sections: The $^{36}\text{S} + ^{208}\text{Pb}$ Reaction

The synthesis and study of the heaviest elements is one of the forefront areas of nuclear science. Most of these studies have involved complete fusion reactions where one can represent the cross section for producing a heavy reaction product, σ_{EVR} , by the equation

$$\sigma_{EVR}(E_{c.m.}) = \sum_{J=0}^{J_{max}} \sigma_{CN}(E_{c.m.}, J) \cdot W_{sur}(E_{c.m.}, J)$$

where σ_{CN} is the complete fusion cross section and W_{sur} is the survival probability of the completely fused system. The complete fusion cross section can be written as

$$\sigma_{CN}(E_{c.m.}) = \sum_{J=0}^{J_{max}} \sigma_{capture}(E_{c.m.}, J) P_{CN}(E_{c.m.}, J)$$

where $\sigma_{capture}(E_{cm}, J)$ is the "capture" cross section at center of mass energy $E_{c.m.}$ and spin J and P_{CN} is the probability that the projectile-target system will evolve inside the fission saddle point to form a completely fused system rather than re-separating (quasifission).

Recently a great deal of attention has been devoted to the possible use of neutron-rich radioactive beams to synthesize heavy nuclei. Such efforts are

motivated by the possibility of enhanced sub-barrier fusion cross sections and increased survival probabilities. To accurately predict the heavy element formation rates in neutron-rich systems, such as those resulting from the use of complete fusion reactions, one needs to know the capture cross sections for very neutron-rich systems. These neutron-rich fusion reactions have been studied using an improved isospin dependent quantum molecular dynamics (IQMD) model [18]. The calculated capture cross sections and barrier heights agreed quantitatively with the experimental data [19-22]. An enhancement of the N/Z ratio in the neck region of the interacting nuclei leads to enhanced sub-barrier fusion cross sections and lowered barrier heights (relative to the semi-empirical systematics [23,24] of capture reactions) for neutron-rich systems.

Most of the reactions involved in these experimental and theoretical determinations of the capture cross sections in neutron rich systems involved radioactive beams. At present, such experiments can suffer from large statistical uncertainties [19] in the measured cross sections due to low beam intensities and, in some cases, uncertainties in the beam energies due to the use of degraders in beam production. We thought it would be useful to study a reaction with stable beams where the relatively high beam intensities lead to low statistical uncertainties in the measured data and where the energies of the projectiles are well-known but also where a large N/Z ratio exists in the composite system. We picked the $^{36}\text{S} + ^{208}\text{Pb}$ reaction and measured the capture fission excitation function.

The capture-fission cross section for the $^{36}\text{S} + ^{208}\text{Pb}$ reaction was measured at the ATLAS accelerator at Argonne National Laboratory. Fission fragments were detected in ten Si surface barrier detectors of area 300 mm^2 each, arranged in a plane at angles $\theta = 75, 85, 95, 110, 120, 130, 140, 150, 160$ and 170° . The resulting center of mass angular distributions were fitted using the standard theory of fission angular distributions [25] and integrated to give the capture cross sections. The measured capture-fission excitation function is shown in Fig. 5.

One possible representation of measured excitation functions, like Fig. 5, is to plot the capture cross section as a function of $1/E_{c.m.}$. The underlying assumption is that the capture cross section may be expressed as,

$$\sigma_{capture} = \pi R_{int}^2 \left(1 - \frac{V_{int}}{E_{c.m.}}\right)$$

where R_{int} is the s-wave interaction barrier radius and V_{int} is the interaction barrier height. The use of this equation implies that all partial waves contributing to the capture cross section have the same barrier radius R_{int} which is probably not true for most reactions. However, in heavy systems, this condition is met and "the effects of varying R_{int} and V_{int} with I largely cancel each other in the cross section formula and the cross section as a whole is relatively insensitive to this I dependence" [26,27].

To test the usefulness of the 1/E method, we have made 1/E plots for the measured excitation functions for 13 well characterized systems which have also been used to construct barrier distributions [28]. We conclude that the $1/E_{cm}$ representation of the data is a good method to extract the average interaction barrier. Use of the $1/E_{c.m.}$ plot for the capture cross sections for the $^{36}\text{S} + ^{208}\text{Pb}$ reaction

gives a value of $V_{int} = 140.4 \pm 1.4$ MeV and $R_{int} = 11.5 \pm 0.2$ fm. In Table 1 we compare this deduced barrier height with various prescriptions and calculations. The Bass model/potential significantly overestimates the barrier height although it should be remarked that this semi-empirical potential is fitted to fusion rather than interaction cross sections. The original prescription of [24] would also give a barrier height that exceeds the measured height. A recent revision of that prescription [29] for neutron-rich systems gives a barrier height in agreement with the measured data. The predicted barrier height from the improved QMD model also correctly describes the measured barrier height.

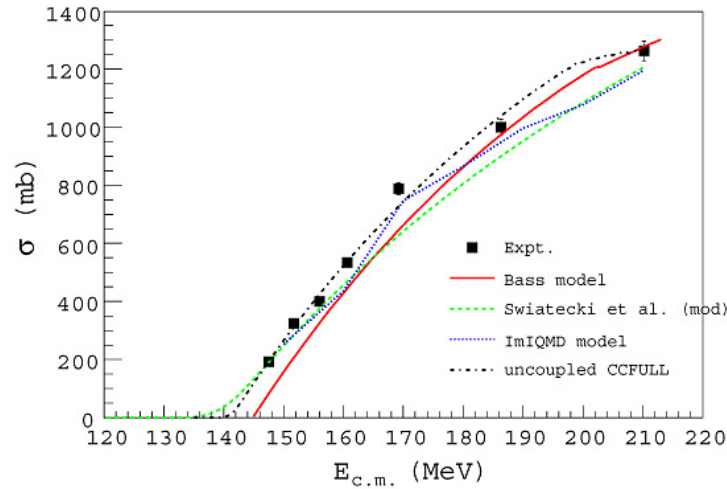


Fig. 5. Measured capture-fission excitation function for the $^{36}\text{S} + ^{208}\text{Pb}$ reaction along with various theoretical predictions.

In Fig. 6 we show the measured values of the interaction barriers as a function of the z parameter (see below) for a large number of neutron rich systems involving stable and radioactive beams where z is defined as

$$z = Z_{projectile}Z_{target}(A_{projectile}^{\frac{1}{3}} + A_{target}^{\frac{1}{3}})^{-1}$$

The best representation of the data is with the modified systematics [29] of Swiatecki et al. The modified QMD model also predicts the observed values. Thus it would seem the cross section enhancements seen previously in studies [19-22] with radioactive beams are well described by both theoretical and semi-empirical models.

Source	V_{int} (MeV)	R_{int} (fm)
Expt.	140.4 ± 1.4	11.5 ± 0.2
Bass	144.8	12.2
Swiatecki et al. (orig.)	142.3	10.5

Swiatecki et al. (mod)	139.7	10.7
Bian	138.1	
CCFULL (uncoupled)	141.2	12.1

Table 1. Interaction barrier heights and radii for the $^{36}\text{S} + ^{208}\text{Pb}$ reaction.

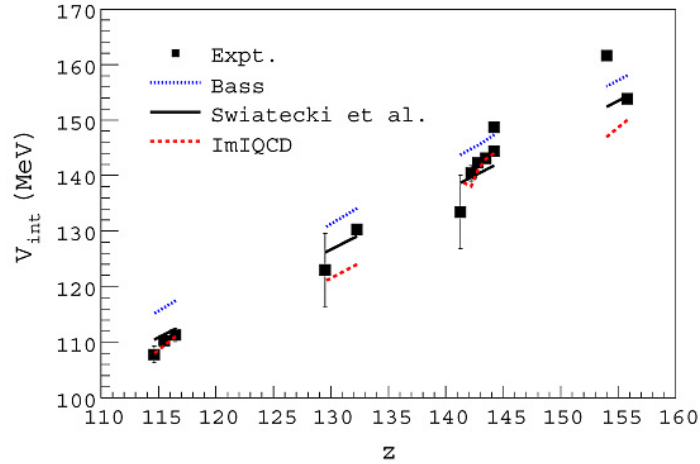


Figure 6 Interaction barrier plotted vs z for reactions involving stable and radioactive beams.

The conclusions and findings of this work are:

- (a) We have measured the capture fission excitation function for the $^{36}\text{S} + ^{208}\text{Pb}$ reaction deducing values of the interaction barrier height, $V_{\text{int}} = 140.5 \pm 0.5$ MeV and the interaction radius of 11.4 ± 0.5 fm.
- (b) By comparing a set of measurements of interaction barrier heights from "distribution of barriers" measurements with $1/E_{\text{c.m.}}$ plots, we conclude the latter technique is a valid way to deduce V_{int} .
- (c) By comparing our results along with deduced interaction barrier heights for all known capture cross section measurements for intermediate mass radioactive beams, we conclude that these barrier heights are in good agreement with recent predictions of an improved QMD model and a modified version of capture cross section systematics of Swiatecki et al.
- (d) The enhanced capture cross sections in very n-rich systems such as those found in radioactive beam induced reactions could lead to substantial improvements in the survival probabilities of heavy nuclei formed in these reactions.

BGS studies of the production of the heaviest elements.

Perhaps the most outstanding development in heavy element science in the past decade has been the successful syntheses of elements 113-118 using hot fusion reactions by the Dubna-Livermore-Oak Ridge group(30,31). However to completely place the new nuclides in the Chart of Nuclides (and to firmly establish the atomic number of the new elements) requires further work. One must unambiguously determine the atomic number of the new nuclides by observing their genetic connection via decay to known nuclei or observing an unambiguous signature (such as K X-ray emission) of the Z of the emitting nucleus. (IUPAC). So far that connection has not been made, although there have been some claims (32).

The heavy element group at the Lawrence Berkeley National Laboratory (Gregorich, Nitsche, et al.) is trying to establish a connection between the “hot fusion” nuclides and the known nuclides. We were invited to assist them in their experiments.

The first study in this effort was the formation of a new isotope of element 114 (and its decay products) using the $^{242}\text{Pu}(^{48}\text{Ca},5n)^{285}114$ reaction. The center of target beam energy was 256 MeV ($E^*=50$ MeV). Two decay chains were observed, one corresponding to the decay of $^{285}114$ and one matching the previously observed decay properties of $^{286}114$. The decay chain of $^{285}114$ included observation of six new nuclides, the alpha emitters $^{285}114$, ^{281}Cn , ^{277}Ds , ^{273}Hs , ^{269}Sg and the spontaneously fissioning ^{265}Rf .

A paper describing this observation has been accepted for publication on Phys. Rev. Letters.

Stern-Gerlach experiment

Without detracting anything from the beautiful difficult experiments to explore the chemistry of the heaviest elements using “one atom at a time” techniques, it has long been realized that these experiments suffer from the need to relate the macroscopic measured quantities such as the enthalpy of adsorption of an atom on a glass or gold surface and the appropriate relativistic quantum chemical calculations of the electron configurations and bonding. The heavy element community has sought to perform an experiment that measures a quantity that can be more directly related to the atomic electron configurations. Some years ago, Hulet and co-workers at LLNL attempted to do a Stern-Gerlach experiment where neutral beams of heavy nuclei are deflected in an inhomogeneous magnetic field thus measuring the spin magnetic moments of the neutral atoms. This experiment failed due to difficulties in forming a beam of neutral atoms and detecting them. In the 15-20 years that have elapsed since this attempt, we have gained substantially more experience in neutralizing beams of ions and detecting those beams. Accordingly a group of scientists from LLNL, LBNL and OSU have commenced discussions aimed at attempting this experiment again at LBNL. The working plan is construct a simplified version of this apparatus, perform experiments with K and/or Ag where neutral beams are easily made, then commence work with Fr. Discussions have been carried out at LBNL to designate this experiment as a priority of the internal heavy element program.

In Table 2, we show the predicted electronic structure and spectroscopic term assignments for the ground states of Fm through Mt. (33).

Element	Electron configuration	Ground state term symbol
Fm	$5f^{12}7s^2$	3H_6
Md	$5f^{13}7s^2$	$^2F_{7/2}$
No	$5f^{14}7s^2$	1S_0
Lr	$5f^{14}7p7s^2$	$^2P_{1/2}$
	$5f^{14}6d7s^2$	$^2D_{3/2}$
Rf	$6d7p7s^2$	3F_4 or 3F_2
	$6d^27s^2$	3F_2
Db	$6d^37s^2$	$^4F_{3/2}$
Sg	$6d^47s^2$	5D_3
Bh	$6d^57s^2$	$^6S_{5/2}$
Hs	$6d^67s^2$	5D_4
Mt	$6d^77s^2$	$^4F_{9/2}$

Table 2. Electronic structure and term assignments for elements 100-109.

For lawrencium, the predicted relativistic and non-relativistic electronic levels are quite different as shown in Figure 7. In the relativistic calculations, the $7p_{1/2}$ electronic level is predicted to lie below the 6d level leading to a different prediction of the electronic group state of the atom. Note that the two possible predicted electronic ground states of Lr will differ in J.

In the classical Stern-Gerlach experiment a beam of silver atoms was passed through an inhomogeneous magnetic field causing a deflection of the atoms in proportion to their magnetic moment and the strength of the magnetic field. The degeneracy of the doublet $S_{1/2}$ ground state was removed by the alignment of the magnetic moment with the magnetic field. This leads to $2J+1$ magnetic substates. For silver, two beams are produced by the inhomogeneous field (corresponding to the $2(1/2) + 1$ magnetic substates.). For any atom there will be $2J+1$ components in the deflected beam, thus allowing the direct measurement of the J of the electronic ground state. For Lr, we would expect either 2 beams or 4 beams depending on the electronic ground state.

The Stern-Gerlach experiment consists of three components, the generation of the atomic beam, the deflection of the beam in a inhomogeneous magnetic field and the detection of the deflected beams. We have adopted the strategy of slowly building up the apparatus, starting with a simple case, the production of a beam of neutral K atoms, deflection of that beam and detection of the neutral K atoms. Following completion of that effort, we will proceed to move to the next step, using the alkali metal Fr (^{221}Fr) produced from a radioactive source where we will introduce the additional step of neutralizing the radioactive ions and then detecting them with particle detectors. All of this will be done at Oregon State University. When this is completed, we intend to move the apparatus of an accelerator facility where ^{221}Fr can be made in a nuclear reaction $^{197}\text{Au}(^{18}\text{O},4n)$. Then we can commence studies of heavy element recoils such as Lr and Rf produced in nuclear reactions.

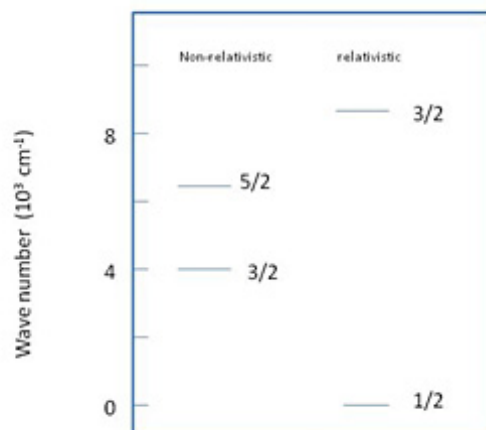


Fig. 7. Comparison of predicted relativistic and non-relativistic energy levels for Lr.

For our studies of the Stern-Gerlach effect with K, we are using a thermal oven as a source of neutral K atoms (see Fig. 8-a). The neutral K atomic beam passes through an inhomogeneous magnetic field of a 10 cm long C-shaped magnet with an intense gradient (1.5 T/cm) (see Fig.8-b). The resulting deflection of the thermal energy K beam is 0.2 mm. At the detector position, the deflection is 2 mm. The K atoms are detected in the traditional hot wire detector with a current amplifier to detect the small beam currents.

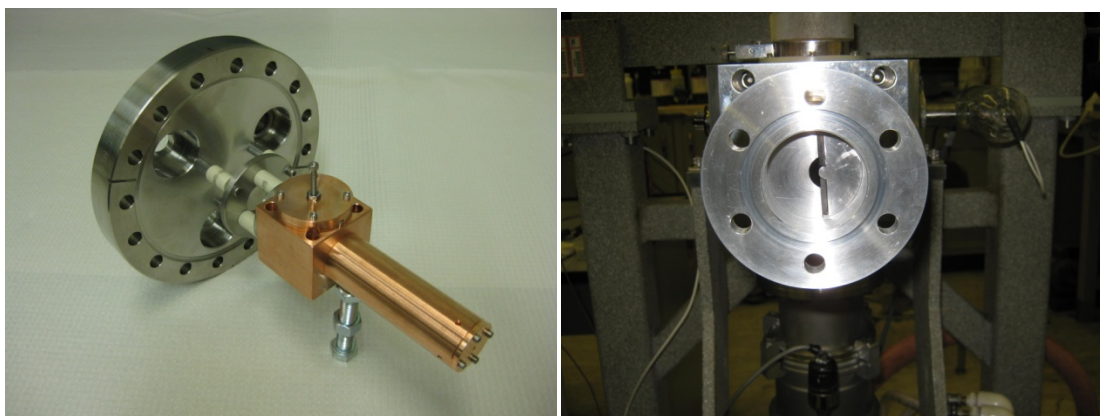


Fig 8. (a) Oven used to generate K beams (b) C magnet used to generate inhomogeneous field.

Inverse Fission

The “inverse fission” experiment [34] is designed to search for and/or set an upper limit on the cross section for the $^{100}\text{Mo} (^{132}\text{Sn}, xn) ^{232-x}\text{U}$ reaction. The preparation for the experiment was basically completed in August, 2008. We have been waiting since then for a resumption of neutron-rich RIB operation at HRIBF following a radiation incident that occurred in August, 2008.

The experiment is to be run in two parts. In the first part, a search for the formation of generic evaporation residues in this reaction is to be carried out using the Shapira ion chamber [35]. Based upon simulations [36] a center-of-target (cot) beam energy of 531 MeV will be used for this part. The intent is to search until an upper limit cross section of 1 mb is reached. In the second part of the experiment, a radiochemical search for a specific evaporation residue, ^{230}U , is carried out. (^{230}U has a unique decay signature and a relatively long half-life, 20.8 days). The cot beam energy for this part of the experiment will be 516 MeV. We anticipate we can set an upper limit on ^{230}U formation at the nb- μb level.

While we have been waiting for beam time at HRIBF, we did a test of the first part of the experiment, the use of the Shapira ion chamber to detect evaporation residues. The test reaction was $^{124}\text{Sn} + ^{100}\text{Mo}$, run at beam energies of 595 and 650 MeV ($E_{\text{cot}} = 578$ and 634 MeV). Upper limit cross sections for evaporation residue formation of 0.2 and 0.5 mb were measured for these energies. HIVAP simulations of these reactions would lead to estimates of the fusion cross sections of 0.0052 and 0.0016 mb, respectively. We have improved the efficiency of the radiochemical separation of ^{230}U from the Al catcher foils until the combined separation/sample preparation efficiency is $> 95\%$. Similar efforts have lowered the background in the alpha counting chambers. A test irradiation is being conducted to test the ^{230}U counting system. The reaction being used is $^{232}\text{Th}(p,3n)^{230}\text{Pa}$ which decays to ^{230}U .

Fusion Studies with Halo/Exotic Nuclei

One of the most active areas of research with radioactive beams is the study of the fusion of weakly bound nuclei, such as the halo nuclei. The central issue is whether the fusion cross section will be enhanced due to the large nuclear size of the halo nucleus or whether fusion-limiting breakup of the weakly bound valence nucleons will lead to a decreased fusion cross section. Most theoretical calculations have dealt with the $^{11}\text{Li} + ^{208}\text{Pb}$ reaction, with a wide variety of outcomes. Figure 9 (taken from a review article of Signorini [37]) shows the range of predictions.

It is clear that a measurement of the fusion excitation function for the $^{11}\text{Li} + ^{208}\text{Pb}$ reaction would be valuable in resolving the differences between the various predictions shown in Figure 9. Our group has been engaged in a deliberate careful approach to measuring the $^{11}\text{Li} + ^{208}\text{Pb}$ fusion excitation function. In TRIUMF experiment 1023, we studied the fusion of ^9Li with ^{70}Zn at ISAC. The results of this study [38] showed a large sub-barrier fusion enhancement for the reaction of ^9Li with ^{70}Zn that was not accounted for by current models of fusion. Zagrebaev et al. [39] found that standard coupled channels calculations along with neutron transfer were not able to describe the observed sub-barrier fusion and postulated “di-neutron transfer” to account for the observed data. Balantekin and Kocak [40] also found that coupled channels calculations including inelastic excitation and one-neutron transfer failed to reproduce the data and suggested the possible formation of a molecular bond accompanied by two-neutron transfer to account for the observed behavior.

Subsequently, with the availability of ISAC2, our group measured the fusion excitation function for the $^9\text{Li} + ^{208}\text{Pb}$ reaction. One observes a sub-barrier fusion

enhancement with ^9Li , the "core" of the ^{11}Li nucleus and a modest suppression of fusion at above barrier energies, compared to coupled channel calculations. The measurement does not agree with the published predictions about this reaction [41].

A proposal to TRIUMF to study the $^{11}\text{Li} + ^{208}\text{Pb}$ reaction was approved and assigned the highest priority. Our preparation for this experiment is summarized on our website [42]

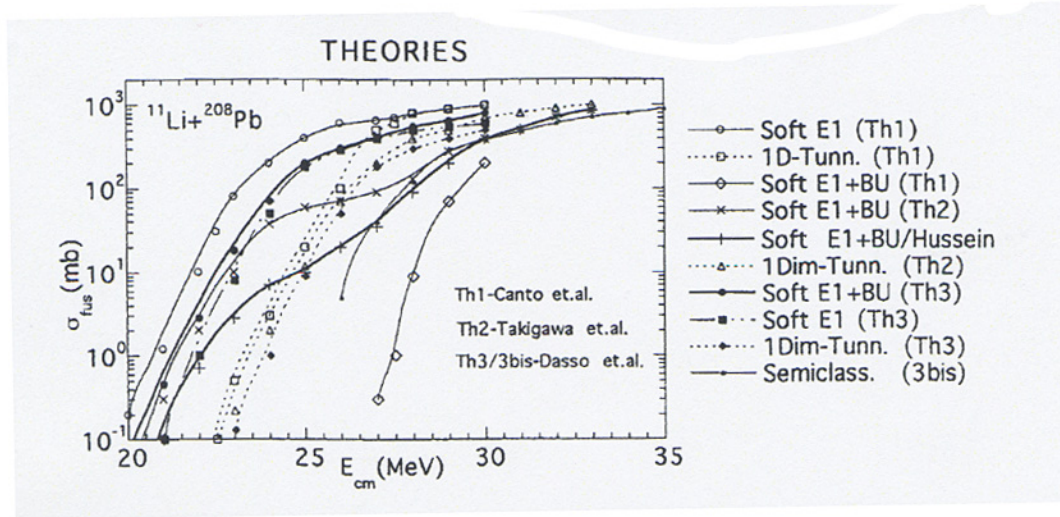


Figure 9. Survey of theoretical predictions of the fusion excitation function for the $^{11}\text{Li} + ^{208}\text{Pb}$ reaction. [37]

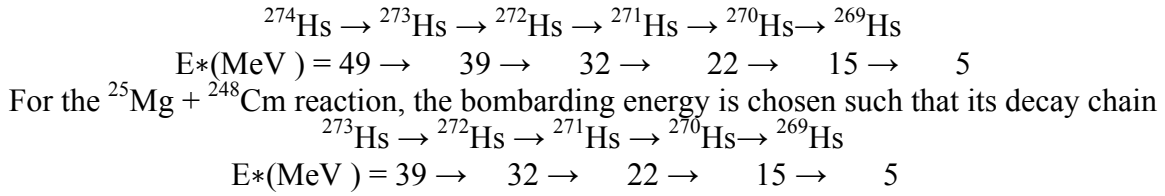
Detailed Studies of Survival Probabilities in Hot Fusion Reactions.

We propose to extend the studies of survival probabilities in hot fusion reactions to study the $^{25,26}\text{Mg} + ^{248}\text{Cm}$ reaction which leads to the formation of Hs isotopes. The evaporation residue yields in this reaction have been studied before [43-45] and cross sections are available for the formation of $^{269,270,271}\text{Hs}$. These evaporation residues are especially interesting because they are at or near the proposed deformed shell at $N=162$, $Z=108$ [46]. As such, they form a perfect laboratory for the study of shell effects on the survival of highly excited nuclei.

There is considerable controversy regarding the appropriate values of W_{sur} and P_{CN} for the $^{248}\text{Cm}(^{26}\text{Mg}, xn)$ systems. For the first chance fission of ^{274}Hs , ($E^*=48.6$ MeV), W_{sur} is estimated to be 9.8×10^{-3} [47], 0.95 [48] or 0.43 [49]. A measurement of W_{sur} for this system will significantly improve our knowledge of survival probabilities in hot fusion reactions leading to the formation of superheavy nuclei.

The methods are to be the same as used on the study of the de-excitation of ^{258}No , [50] i.e., to form ^{274}Hs ($E^*=48.6$ MeV) via the $^{26}\text{Mg} + ^{248}\text{Cm}$ reaction and to form ^{273}Hs ($E^*=39.3$ MeV) using the $^{25}\text{Mg} + ^{248}\text{Cm}$ reaction and to measure the fission associated neutron multiplicities in these reactions. The logic behind the use of cross bombardments is given below.

In the reaction $^{26}\text{Mg} + ^{248}\text{Cm}$, we detect neutrons from the decay chain



energetically matches the corresponding elements of the ${}^{274}\text{Hs}$ chain, allowing a direct comparison of the neutrons emitted solely from that nucleus avoiding the difficulties inherent to other, model-dependent analysis methods. It is straightforward to demonstrate that

$$\left(\frac{\Gamma_n}{\Gamma_{tot}} \right)_1 = \frac{{}^{274}\nu_{pre}}{1 + {}^{273}\nu_{pre}}$$

A thin-walled Al scattering chamber will be used along with a new array of BC-501 scintillators to detect the neutrons. Fission fragments will be detected using semiconductor detectors. Neutron spectra will be deduced from time of flight data with the use of pulse-shape discrimination to separate neutrons and gamma rays. Because one is measuring the properties of the first and second chance fission events, the relevant cross sections are the fusion-fission cross sections for these reactions (of several hundred mb). The asymmetry of the reacting system ($Z_p Z_t = 1152$) should insure no complications from the effects of quasifission [51]. Also, a recent measurement of Itkis et al. [52] showed the ${}^{26}\text{Mg} + {}^{248}\text{Cm}$ reaction “to be a pure fusion-fission process”. From these multiplicities, angular correlations and energy spectra, one will extract values of the pre-fission neutron multiplicities, ν_{pre} , and the survival probability, $((\Gamma_n)/(\Gamma_{tot}))$, for the first chance fission of ${}^{274}\text{Hs}$ ($E^*=48.6$ MeV). Comparison of these data and the evaporation residue data with modern calculations of survival probabilities in these multiple chance fission reactions should allow us to understand the de-excitation of these highly excited nuclei in systems where there are important ground state shell effects.

In preparation for this experiment, we have done extensive simulations of the detector response functions and efficiencies using MCNP5 and SCINFUL. A typical detector efficiency function is shown in Figure 10 along with a measured fission neutron spectrum for ${}^{252}\text{Cf}$ spontaneous fission. The spectrum has been decomposed into contributions from the two fission fragments moving at angles θ and $\pi-\theta$.

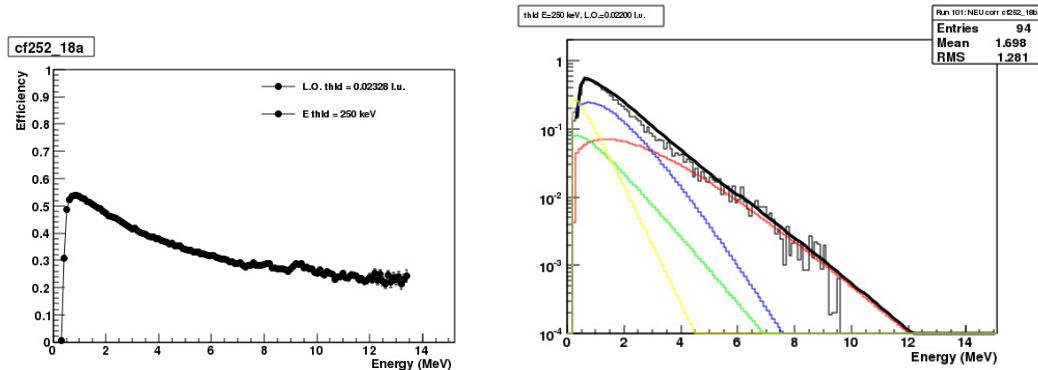


Figure 10. (a) Simulated efficiency function for BC501A detector. (b) Measured ^{252}Cf spontaneous fission neutron spectrum decomposed into contributions from the two fission fragments

Anticipated Unexpended Funds We do not anticipate any unexpended funds as of 12/31/10.

References

1. E. Kozulin, et al., Phys. Lett. B 686, 227 (2010).
2. Y.T. Oganessian, et al., Phys. Rev. C 79, 024603 (2009).
3. See G.T. Seaborg and W. Loveland, The Elements Beyond Uranium (Wiley, New York, 1990) for a review of these data.
4. V.I. Zagrebaev, Y.T. Oganessian, M.G. Itkis and W. Greiner, Phys. Rev. C73, 031602(R) (2006).
5. V. Zagrebaev, and W. Greiner, J. Phys. G 34, 1 (2007).
6. V. Zagrebaev, and W. Greiner, J. Phys. G 31, 825 (2005).
7. V. Zagrebaev and W. Greiner, J. Phys. G 35, 125103 (2008).
8. V. Zagrebaev and W. Greiner, Phys. Rev. Lett 101, 12270 (2008)
9. V. Zagrebaev and W. Greiner, CP1098, FUSION08: New Aspects of Heavy Ion Collisions Near the Coulomb Barrier, K.E. Rehm, B.B. Back, H. Esbensen, and C.J. Lister, ed., (AIP, New York, 2009) pp326-333
10. V. Zagrebaev and W. Greiner, Nucl. Phys. A 834, 366c (2010).
11. V. Zagrebaev and W. Greiner, Phys. Rev. C78, 034610 (2008).
12. V. Zagrebaev and W. Greiner, Russ. Chem. Rev. 78, 1089 (2009).
13. V. Zagrebaev and W. Greiner, J. Phys. G 34, 2265 (2007).
14. NAS-NS-3040, The radiochemistry of lead, W.M. Gibson, USAEC. 1961, Procedure 11.
15. K. Aleklett, J. O. Liljenzin, and W. Loveland, J. Radioanal. Nucl. Chem. 193, 187 (1996).
16. G. Friedlander, J.W. Kennedy, E. S. Macias, and J. M. Miller, Nuclear and Radiochemistry, 3rd Edition (Wiley, New York, 1981) p191.
17. D.J. Morrissey, W. Loveland, M. de Saint-Simon, and G.T. Seaborg, Phys. Rev. C 21, 1783 (1980).
18. Bao-An Bain, Feng-Shou Zhang, and Hong-Yu Zhou, Nucl. Phys. A 829, 1 (2009).
19. W. Loveland, D. Peterson, A. M. Vinodkumar, P. H. Sprunger, D. Shapira, J. F. Liang, G.A. Souliotis, D. J. Morrissey, and P. Lofy, Phys. Rev. C74, 044607(2006).
20. K.E. Zyranski, W. Loveland, G. A. Souliotis, D. J. Morrissey, C. F. Powell, O. Batenkov, K. Aleklett, R. Yanez, and I. Forsberg, Phys. Rev. C63, 024615 (2001).

21. Y.X. Watanabe, et al., Eur. Phys. J. A10, 373 (2001).
22. J.F. Liang, et al., Phys. Rev. C75, 054607 (2007).
23. K. Siwek-Wilczynska, and J. Wilczynski, Phys. Rev. C 64, 024611 (2001)
24. W.J. Swiatecki, K. Siwek-Wilczynska, and J. Wilczynski, Phys. Rev. C 71, 014602 (2005).
25. B. B. Back, et al., Phys. Rev. C 32, 195 (1985)
26. U. Mosel in *Treatise on Heavy Ion Science*, Vol. 2, D.A. Bromley ed. (Plenum, New York, 1984) pp 3-49
27. K. Nagatani and J.C. Peng, Phys. Rev. C 19, 747 (1979).
28. N. Rowley, G.R. Satchler, and P.H. Stelson, Phys. Lett. B 254, 25 (1991).
29. K. Siwek-Wilczynska (private communication).
30. Y. Oganessian, J. Phys. G: Nucl. Part. Phys. 34, R165 (2007).
31. Y.T. Oganessian, et al., Phys. Rev. Lett. 104, 142502 (2010).
32. R. Eichler, D.A. Shaughnessy, P.A. Wilk, J.M. Kenneally, M.A. Stoyer, and J.F. Wild, *Mendelev Communications* 15, 1 (2005).
33. B. Fricke and J.T. Waber, *Actinide Rev.* **1**, 433 (1971).
34. W. Loveland, *J. Radioanal. Nucl. Chem.*, **276**, 519 (2008).
35. D. Shapira, et al., *Nucl. Instru. Meth. Phys. Res.* **A551**, 330 (2005).
36. W. J. Swiatecki, K. Siwek-Wilczynska, and J. Wilczynski, Phys. Rev. C 78, 054604 (2008).
37. C. Signorini, *J. Phys. G: Nucl. Part. Phys* 23, 1235 (1997).
38. W. Loveland, et al., Phys. Rev. C 74, 064609 (2006).
39. V. I. Zagrebaev, V.V. Samarin, and W. Greiner, Phys. Rev. C 75, 035809 (2007).
40. A.B. Balantekin, and G. Kocak, *AIP Conference Proceedings* 1072, 289 (2008).
41. N. Takigawa, M. Kuratani, and H. Sagawa, Phys. Rev. C 47, R2470 (1993).
42. <http://holme.radiationcenter.oregonstate.edu/Li11Pb208>
43. A. Turler, et al., Eur. Phys. J A **17**, 505 (2003).
44. J. Dvorak, et al., Phys. Rev. Lett. **97**, 242501 (2006).
45. J. Dvorak, et al. Phys. Rev. Lett. **100**, 132503 (2008)
46. Z. Patyk, et al., *Nucl. Phys.* **A502**, 591 (1989); *Nucl. Phys.* **A533**, 132 (1991)
47. W.J. Swiatecki, et al., Phys. Rev. C71, 014602 (2005), K. Siwek-Wilczynska (private communication)
48. <http://nrv.jinr.ru/nrv/>
49. W. Reisdorf and M. Schaedel, *Zeit. Phys.* **A343**, 47 (1992).
50. D. Peterson et al., Phys. Rev. C **79**, 044607 (2009)
51. K. E. Rehm, *Ann. Rev. Nucl. Part Sci.* **41**, 429 (1991).
52. M.G. Itkis, et al, *Nucl Phys. A* **834**, 374c (2010).